Available online at www.eccomasproceedia.org
Eccomas Proceedia SMART (2025) 53-62

ECCOMAS
Proceedia

XI ECCOMAS Thematic Conference on Smart Structures and Materials - SMART 2025
M. Krommer, M. Nader and M. Schagerl (Eds)

Received: 9 April 2025 / Revised: 1 October 2025 / Accepted: 3 October 2025

Magnetostrictive Shunt versus Piezoelectric Shunt: A Comparison

Marta Berardengo, Marco Mercato, Stefano Manzoni

Abstract. This paper treats the use of magnetostrictive shunt to the aim of vibration control when a primary system is excited by an external disturbance. It is shown that when the primary system is coupled with an magnetostrictive element surrounded by a coil, and this coil is shunted with a proper electric impedance, vibration reduction is achieved. To model the coupled system, an approach already used for piezoelectric shunt is employed, defining similar non-dimensional parameters which are then shown to drive the attenuation performance and the shunt tuning, exactly as for piezoelectric shunt. This model constitutes an improvement compared to the models available in the literature and shows that a strict parallelism exists between the two considered types of shunt control. Nevertheless, when practical applications are considered, it comes out that some adjustments are needed for the model of magnetostrictive shunt, mainly due to the magnetic losses in the shunted coil. This makes magnetostrictive shunt and piezoelectric shunt slightly different, and the paper proposes a possible upgrade for the model of magnetostrictive system. All the theoretical results related to magnetostrictive shunt are validated by means of a tailored set-up, focusing on the case of mono-modal control and using both resistive and resonant shunt. The work also defines which are the main limits of magnetostrictive shunt compared to piezoelectric shunt, and it resulted that the main limitations are primarily related to the inability to achieve optimal tuning when low frequency modes need to be attenuated. The proposed model of magnetostrictive shunt can also be used for other applications, such as, e.g., structural health monitoring.

Key words: Vibration control, Magnetostrictive shunt, Piezoelectric shunt, Resistive shunt, Resonant shunt

Marta Berardengo & Marco Mercato
Department of Mechanical, Energy, Management and Transportation Engineering, Universitá degli Studi di Genova, Via all'Opera Pia, 15a - 16145 Genoa, Italy
e-mail: marta.berardengo@unige.it

Stefano Manzoni
Department of Mechanical Engineering, Politecnico di Milano, Via La Masa, 1 - 20156 Milan, Italy, e-mail: stefano.manzoni@polimi.it

ISSN:3078-543X. Published by Eccomas Proceedia.
Peer-review under responsibility of the organizing committee of SMART 2025.
doi: 10.7712/150125.13615.201001

1 INTRODUCTION

The use of intelligent materials in the field of vibration control is gaining more and more attention because of the advantages provided by employing these types of materials. A very attractive approach when using intelligent materials is the so called shunt control where a proper electric network is connected to the material, obtaining a significant control action (e.g., [1, 2, 3, 4]). Different successful real applications are already described in the literature, especially considering piezoelectric shunt (e.g., [5, 6, 7, 8]). Magnetostrictive (MS) shunt is less considered in the literature but recently different works have analysed it [9, 10, 11, 12], evidencing its capability in providing good control performances.

This paper is aimed at showing similarities and differences among MS shunt and the piezoelectric shunt. Being the latter largely studied, the final aim is to evidence how control strategies developed for piezoelectric shunt can be used in the context of the MS shunt. Furthermore, the similarities between piezoelectric and MS shunt will be also useful for applying MS shunt in the context of structural health monitoring, since piezoelectric shunt has already been proven to be a reliable approach in this context [13].

The paper is structured as follows: Section 2 describes the models of the two shunt types, evidencing the similarities, then Section 3 presents some numerical simulations for analysing the control performance of MS shunt. Finally, Section 4 will discuss some practical issues which must be accounted for when using MS shunt, which are instead not significant in the context of piezoelectric shunt.

2 SHUNT MODELS

The system considered is the generic multi-degree-of-freedom system depicted in Fig. 1. The green rectangle named 'intelligent material' can be either a piezoelectric element or an MS element (surrounded by a coil).

Writing the equations of motion of the system and the equation of the electrical part, passing then in modal coordinates q_i (where q_i is the modal coordinate for the i-th mode, with $i = 1, .., G$), the following equations are obtained for the piezoelectric case [14, 15]

$$\ddot{q}_i(t) + 2\xi_i\omega_i\dot{q}_i(t) + \omega_i^2 q_i(t) - \chi_i V(t) = F_i(t), \quad \forall i \in \{1, \cdots, G\} \tag{1}$$

$$C_\infty V(t) - Q(t) + \sum_{i=1}^{G} \chi_i q_i(t) = 0 \tag{2}$$

and for the MS case [9]

$$\ddot{q}_i(t) + 2\xi_i\omega_i\dot{q}_i(t) + \omega_i^2 q_i(t) - \theta\phi_{i,1} I(t) = F_i(t), \quad \forall i \in \{1, \cdots, G\} \tag{3}$$

$$V(t) = R_c I(t) + L_c \dot{I}(t) + \bar{\theta} \sum_{i=1}^{G} \phi_{i,1}\dot{q}_i(t) \tag{4}$$

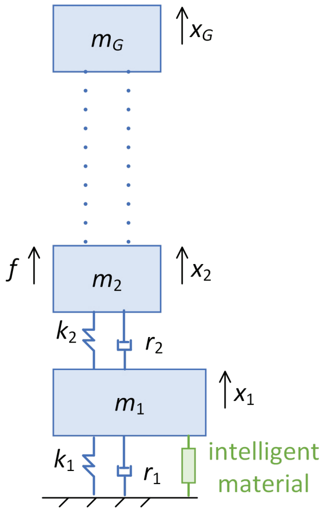

Figure 1: Schematic of a multi-degree-of-freedom system equipped with an intelligent material and excited by an external disturbance f.

where F_i is the modal force, ω_i is the i-th eigenfrequency (with either the piezoelectric element short-circuited or the coil open-circuited for the MS case), ξ_i is the associated non-dimensional damping ratio, V is either the voltage between the electrodes of the piezoelectric element or between the terminals of the coil, Q is the charge in one of the electrodes of the piezoelectric element ($-Q$ in the other), I is the current flowing in the coil, t is time, C_∞ is the capacitance of the piezoelectric element at constant strain (i.e., at infinite frequency, blocked capacitance), χ_i is a coupling coefficient describing the energy transfer between the i-th mode and the electrical part of the system based on the piezoelectric element, θ and $\bar{\theta}$ are constants depending on characteristics of the MS element and the associated coil, L_c is the coil inductance at constant strain, R_c is the associated inherent resistance of the coil, and, finally, $\phi_{i,1}$ is the eigenvector component of the i-th mode for the first degree of freedom (normalised to the unit modal mass and with the coil open-circuited).

To further elaborate equations (1) to (4) and show the similarities between the two types of shunt, a single-degree-of-freedom (SDOF) reduction can be performed.

According to [16], the SDOF reduction for the piezoelectric case leads to the following equations describing the dynamics of the system for $\Omega \simeq \omega_i$ (where Ω is the angular frequency):

$$\ddot{q}_i(t) + 2\xi_i\omega_i\dot{q}_i(t) + \omega_i^2 q_i(t) - \chi_i V t) = F_i(t) \tag{5}$$

$$C_{\mathrm{p},i}V(t) - Q(t) + \chi_i q_i(t) = 0 \tag{6}$$

where $C_{\mathrm{p},i}$ is the modal capacitance of the i-th mode, which allows accounting for the contribution of the out-of-band modes [17]. Considering the MS case, according to [9], the equations of the SDOF case are:

$$\ddot{q}_i(t) + 2\xi_i\omega_i\dot{q}_i(t) + \omega_i^2 q_i(t) - \theta\phi_{i,1}I(t) = F_i(t) \tag{7}$$

$$V(t) = R_\mathrm{c}I(t) + L_i\dot{I}(t) + \bar{\theta}\phi_{i,1}\dot{q}_i(t) \tag{8}$$

where L_i is the modal inductance of the i-th mode [9] and, also in this case, it is a quantity used to take into account the contribution of the out-of-band modes.

Equations (5) and (6) can be used to find the frequency response function (FRF) $H_i(\mathrm{j}\Omega) = q_i^\mathrm{f}/F_i^\mathrm{f}$ (superscript f indicates that the quantity is transformed in the frequency domain, while j is the imaginary unit) in case of specific shunt impedances Z_sh for piezoelectric shunt, by mixing them with the considered expression of Z_sh. The same can be performed for MS shunt with Eqs. (7) and (8). To evidence the similarities between piezoelectric and MS shunts, resistive and resonant shunts are considered, also because they are the most used types of shunt impedances in piezoelectric shunt.

2.1 Resistive shunt

When the shunt impedance is made from a simple resistance R, the FRF H_i can be expressed as:

$$H_i(\mathrm{j}\Omega) = \frac{1 + \mathrm{j}\tau\Omega}{\omega_i^2 - \Omega^2(1 + 2\xi_i\omega_i\tau) + \mathrm{j}\Omega(\hat{\omega}_i^2 + 2\xi_i\omega_i - \tau\Omega^2)} \tag{9}$$

where $\tau = C_{\mathrm{p},i}R$ for piezoelectric shunt while $\tau = L_i/(R_\mathrm{c} + R) = L_i/R_\mathrm{tot}$ for MS shunt. Furthermore, $\hat{\omega}_i$ is the i-th eigenfrequency of the system with either the piezoelectric element open-circuited or the coil surrounding the MS element short-circuited.

Since the FRF in case of resistive shunt has the same form for the two shunt types, the way to optimise the value of R for controlling the i-th mode can be directly derived by the theory of piezoelectric shunt: the optimal value of τ (named τ_opt) for controlling the i^th mode is equal to [16]:

$$\tau_\mathrm{opt} = \sqrt{\frac{2}{\hat{\omega}_i^2 + \omega_i^2}} \tag{10}$$

Then, it is possible to calculate R using the corresponding link between τ and R for the considered shunt type, having estimated in advance the value of either $C_\mathrm{p,i}$ or L_i. The corresponding attenuation A_dB of the FRF amplitude peak is equal to [1]:

$$A_\mathrm{dB} = 20\log_{10}\frac{k_i^2 + 2\sqrt{2}\xi_i\sqrt{2 + k_i^2}}{4\xi_i\sqrt{1 - \xi_i^2}} \tag{11}$$

Here, the quantity k_i must be introduced. It is the modal coupling coefficient and it can be estimated in both the shunt types as [9]:

$$|k_i| \simeq \sqrt{\frac{\hat{\omega}_i^2 - \omega_i^2}{\omega_i^2}} \tag{12}$$

2.2 Resonant shunt

This subsection treats the case in which Z_{sh} is made from the series of a capacitance C and a resistance R for MS shunt and from the parallel between an inductance L and a resistance R for piezoelectric shunt.

In both the cases, the resulting FRF H_i is equal to:

$$H_i(\mathrm{j}\Omega) = \frac{-\Omega^2 + 2\mathrm{j}\xi_{\mathrm{e}}\omega_{\mathrm{e}}\Omega + \omega_{\mathrm{e}}^2}{\Omega^4 - \Omega^2 P_i + \omega_{\mathrm{e}}^2\omega_i^2 + 2\mathrm{j}\Omega p_i} \tag{13}$$

with

$$P_i = \omega_{\mathrm{e}}^2 + 4\xi_{\mathrm{e}}\xi_i\omega_{\mathrm{e}}\omega_i + \hat{\omega}_i^2 \tag{14}$$

$$p_i = [\xi_{\mathrm{e}}\omega_{\mathrm{e}}(\omega_i^2 - \Omega^2) + \xi_i\omega_i(\omega_{\mathrm{e}}^2 - \Omega^2)] \tag{15}$$

Furthermore, ω_{e} and ξ_{e} for piezoelectric shunt are

$$\omega_{\mathrm{e}}^2 = 1/(C_{\mathrm{p},i}L) \tag{16}$$

$$\xi_{\mathrm{e}} = \frac{1}{2R}\sqrt{\frac{L}{C_{\mathrm{p},i}}} \tag{17}$$

and, for MS shunt, they are:

$$\omega_{\mathrm{e}}^2 = 1/(L_iC) \tag{18}$$

$$\xi_{\mathrm{e}} = \frac{R + R_{\mathrm{c}}}{2}\sqrt{\frac{C}{L_i}} = \frac{R_{\mathrm{tot}}}{2}\sqrt{\frac{C}{L_i}} \tag{19}$$

It is easy to demonstrate that a shunt impedance made from the parallel of a R and C for MS shunt leads to the same FRF related to a shunt impedance made from the series of R and L for piezoelectric shunt. This implies the possibility of finding optimal values for the shunt components and the corresponding attenuation performances with the approaches developed for piezoelectric shunt (see [18, 19]).

3 NUMERICAL ANALYSIS

The above formulations allows deriving the attenuation A_{dB} for both resonant and resistive shunt. As in the case of piezoelectric shunt, MS shunt offers attenuation performances depending on ξ_i and k_i. Figure 2 shows the resulting curves, which evidence the larger attenuation provided by resonant shunt.

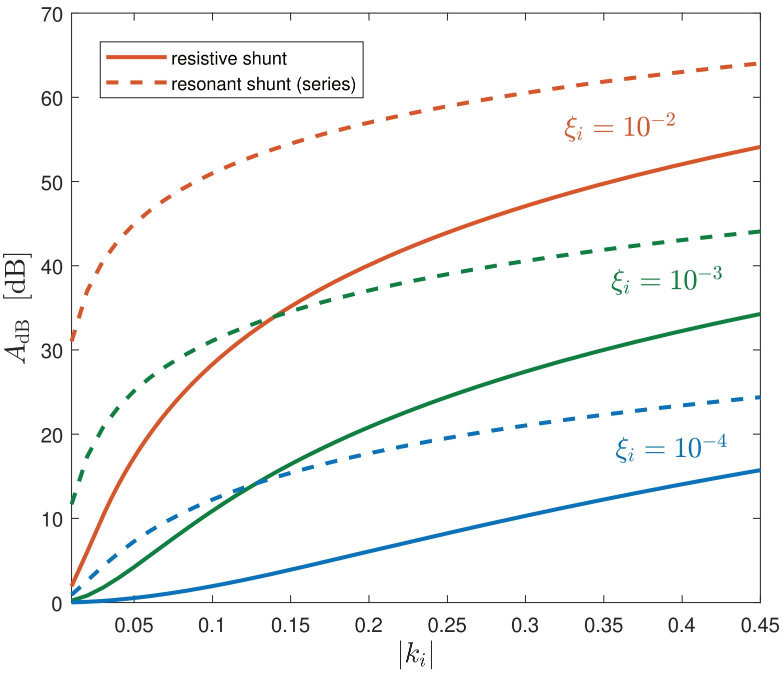

Figure 2: Trend of the attenuation (reduction of peak amplitude on a given mode) A_{dB} as function of the value of $|k_i|$ and for three different ξ_i values for resistive and resonant (series connection between R and C) MS shunt.

Furthermore, the above treatment allows deriving the optimal resistance values for piezoelectric and MS shunts in case of either resistive or resonant shunt. Figure 3a shows the trend of the optimal resistance for resistive shunt for different ω_i and $|k_i|$ values, while Fig. 3b provides the same information for resistive shunt. It results that the resistance values are much larger for piezoelectric shunt compared to MS shunt, making piezoelectric shunt better in terms of ease of implementation. Moreover, the value of the optimal resistance for MS shunt must account also for R_{c}. At low frequency, the optimal resistance can be larger than the value of R_{c}, implying the impossibility of reaching an optimal tuning of the shunt impedance.

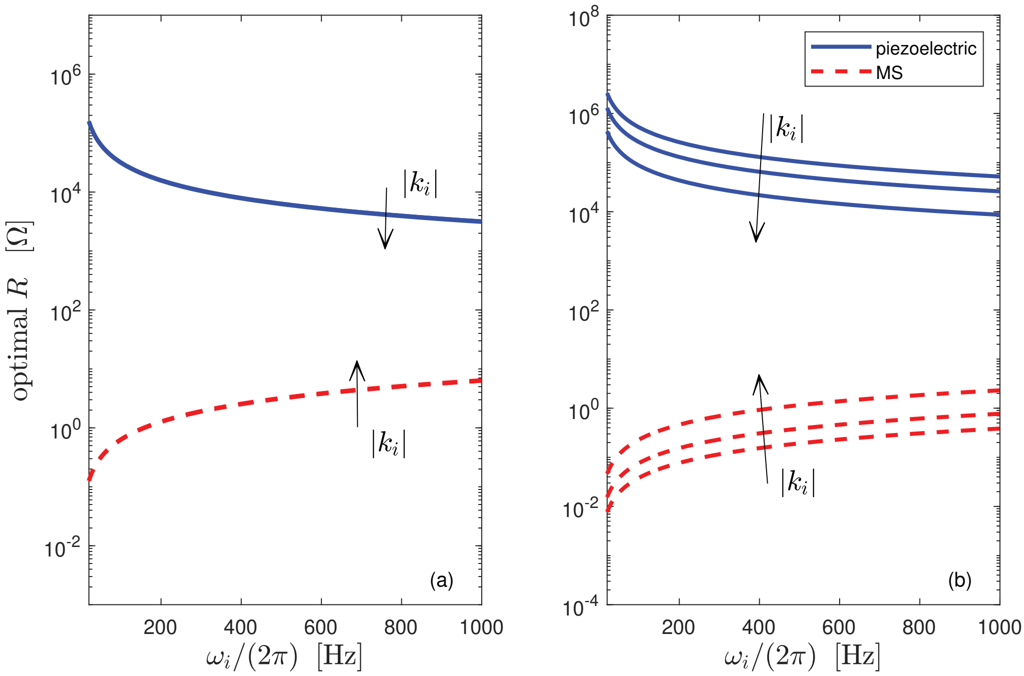

Figure 3: Trend of the optimal resistance as function of ω_i and for three different $|k_i|$ values (i.e., 0.05, 0.1 and 0.3) for resistive (a) and resonant (b) shunt in both piezoelectric and MS shunt. The shunt components are connected in series for MS shunt, and in parallel for piezoelectric shunt.

4 MAIN DIFFERENCE BETWEEN PIEZOELECTRIC AND MS SHUNT

The main difference between piezoelectric and MS shunt is related to the fact that the value of the modal inductance L_i must be adjusted to take into account the effect of magnetic losses of the coil. Indeed, considering as an example the equivalent inductance (measured on a set-up in the labs of Politecnico di Milano) of magnetostrictive material (obtained by inserting current in the coil and measuring the consequent voltage at the pins of the coil), a decreasing trend due to losses is present. When SDOF reductions are considered, it is possible to adjust the value of L_i as

$$\tilde{L}_i = L_i - \eta\omega_i \tag{20}$$

where η is a constant describing the descending trend around ω_i. A more detailed description of the problem is available in [9].

Conversely, the value of $C_{\mathrm{p},i}$ does not need any adjustment.

5 CONCLUSION

The paper has dealt with the parallelism between piezoelectric and MS shunt, showing that there is a common mathematical approach for describing both the approaches. The paper has also evidenced that there are some limits and issues (e.g., magnetic losses) associated to MS shunt which are not observed for piezoelectric shunt. The developed model of MS shunt will be useful not only for vibration control purposes but also for structural health monitoring applications of MS materials.

ACKNOWLEDGMENTS

This research has been supported by the project ”CHIMERA? - is there a CHance that Indexes and Measurements of the energy conversion Efficiency Reveal system Alterations?” funded by the European Union – Next Generation EU, M4C2 I1.1, through Progetti di Rilevante Interesse Nazionale (PRIN) 2022, grant n. 20225PKHWJ (CUP: D53D23003060006).

REFERENCES

[1] O. Thomas, J. Ducarne, and J. Deü, “Performance of piezoelectric shunts for vibration reduction,” *Smart Materials and Structures*, vol. 21, no. 1, 2012, 015008.

[2] J. D. Richardt, B. Lossouarn, J. Høgsberg, and J.-F. Deü, “Calibration of multiple shunted piezoelectric transducers with correction for residual modes and shunt interactions,” *JVC/Journal of Vibration and Control*, vol. 31, no. 1-2, p. 24 – 36, 2025.

[3] T. Wang, J. Dupont, and J. Tang, “On integration of vibration suppression and energy harvesting through piezoelectric shunting with negative capacitance,” *IEEE/ASME Transactions on Mechatronics*, vol. 28, pp. 2621 – 2632, 2023.

[4] P. Gardonio and G. K. Rodrigues, “Shunted piezoelectric patch adaptive vibration absorber set to maximise electric power absorption: A comparison between parallel and series rl-shunts,” *JVC/Journal of Vibration and Control*, vol. 31, no. 1-2, p. 37 – 50, 2025.

[5] H. Sun, Z. Yang, K. Li, B. Li, J. Xie, D. Wu, and L. Zhang, “Vibration suppression of a hard disk driver actuator arm using piezoelectric shunt damping with a topology-optimized pzt transducer,” *Smart Materials and Structures*, vol. 18, 2009, 065010.

[6] Y. Watine, B. Lossouarn, C. Gabillet, J.-A. Astolfi, and J.-F. Deü, “Mitigation of hydrofoil torsional flow induced vibrations by resonant piezoelectric shunt,” *Ocean Engineering*, vol. 313, 2024, 119598.

[7] B. Zhou, F. Thouverez, and L. D., “Vibration reduction of mistuned bladed disks by passive piezoelectric shunt damping techniques,” *AIAA Journal*, vol. 52, pp. 1194–1206, 2014.

[8] K. Zhou and Z. Hu, "Vibration suppression on the composite laminated plates subjected to aerodynamic and harmonic excitations based on the nonlinear piezoelectric shunt damping," *Applied Mathematical Modelling*, vol. 121, pp. 134–165, 2023.

[9] M. Berardengo, M. Mercato, and S. Manzoni, "Magnetostrictive shunt for vibration control and isolation: model, characteristics and similarities with piezoelectric shunt," *Smart Materials and Structures*, vol. 34, no. 1, 2025, 015043.

[10] Z. Deng, J. J. Scheidler, V. M. Asnani, and M. J. Dapino, "Shunted magnetostrictive devices in vibration control," *Smart Materials and Structures*, vol. 29, no. 10, 2020, 105007.

[11] E. Fukada, M. Date, and K. Sekigawa, "Vibration control by magnetostrictive actuator coupled with negative inductance circuits," *Japanese Journal of Applied Physics*, vol. 42, no. 11, pp. 7124–7128, 2003.

[12] J. J. Scheidler and V. M. Asnani, "Validated linear dynamic model of electrically-shunted magnetostrictive transducers with application to structural vibration control," *Smart Materials and Structures*, vol. 26, no. 3, 2017, 035057.

[13] M. Berardengo, M. Brambilla, A. Codina, N. Schena, and S. Manzoni, "Piezoelectric coupling as a feature sensitive to structural alterations," *Mechanical Systems and Signal Processing*, vol. 224, 2025, 112012.

[14] O. Thomas, J.-F. Deü, and J. Ducarne, "Vibration of an elastic structure with shunted piezoelectric patches: efficient finite-element formulation and electromechanical coupling coefficients," *International Journal of Numerical Methods in Engineering*, vol. 80, no. 2, pp. 235–268, 2009.

[15] J. Ducarne, O. Thomas, and J. Deü, "Placement and dimension optimization of shunted piezoelectric patches for vibration reduction," *Journal of Sound and Vibration*, vol. 331, no. 14, pp. 3286–3303, 2012.

[16] M. Berardengo, O. Thomas, C. Giraud-Audine, and S. Manzoni, "Improved resistive shunt by means of negative capacitance: new circuit, performances and multi mode control," *Smart Materials and Structures*, vol. 25, 2016, 075033.

[17] M. Berardengo, S. Manzoni, J. Høgsberg, and M. Vanali, "Vibration control with piezoelectric elements: The indirect measurement of the modal capacitance and coupling factor," *Mechanical Systems and Signal Processing*, vol. 151, 2021, 107350.

[18] K. Yamada, H. Matsuhisa, H. Utsuno, and K. Sawada, "Optimum tuning of series and parallel lr circuits for passive vibration suppression using piezoelectric elements," *Journal of Sound and Vibration*, vol. 329, no. 24, pp. 5036–5057, 2010.

[19] M. Berardengo, S. Manzoni, O. Thomas, and M. Vanali, “Guidelines for the layout and tuning of piezoelectric resonant shunt with negative capacitances in terms of dynamic compliance, mobility and accelerance,” *Journal of Intelligent Material Systems and Structures*, vol. 32, no. 17, p. 2092 – 2107, 2021.